Cell. Mol. Life Sci. (2009) 66:3979–3991
DOI 10.1007/s00018-009-0158-4

Cellular and Molecular Life Sciences

RESEARCH ARTICLE

Inhibition of cholesterol recycling impairs cellular PrP^{Sc} propagation

Sabine Gilch · Christian Bach · Gloria Lutzny · Ina Vorberg · Hermann M. Schätzl

Received: 4 September 2009 / Accepted: 14 September 2009 / Published online: 13 October 2009

Abstract The infectious agent in prion diseases consists of an aberrantly folded isoform of the cellular prion protein (PrP^{c}), termed PrP^{Sc}, which accumulates in brains of affected individuals. Studies on prion-infected cultured cells indicate that cellular cholesterol homeostasis influences PrP^{Sc} propagation. Here, we demonstrate that the cellular PrP^{Sc} content decreases upon accumulation of cholesterol in late endosomes, as induced by NPC-1 knockdown or treatment with U18666A. PrP^{c} trafficking, lipid raft association, and membrane turnover are not significantly altered by such treatments. Cellular PrP^{Sc} formation is not impaired, suggesting that PrP^{Sc} degradation is increased by intracellular cholesterol accumulation. Interestingly, PrP^{Sc} propagation in U18666A-treated cells was partially restored by overexpression of rab 9, which causes redistribution of cholesterol and possibly of PrP^{Sc} to the trans-Golgi network. Surprisingly, rab 9 overexpression itself reduced cellular PrP^{Sc} content, indicating that PrP^{Sc} production is highly sensitive to alterations in dynamics of vesicle trafficking.

Keywords Cholesterol · Recycling · Prion · PrP · NPC-1 · Rab 9

Electronic supplementary material The online version of this article (doi:10.1007/s00018-009-0158-4) contains supplementary material, which is available to authorized users.

S. Gilch · C. Bach · G. Lutzny · I. Vorberg · H. M. Schätzl (✉)
Institute of Virology, Prion Research Group,
Technische Universität München, Trogerstr. 30,
81675 Munich, Germany
e-mail: schaetzl@lrz.tum.de

Introduction

Spongiform neurodegeneration is a pathological hallmark of prion diseases, a group of rare and inevitably fatal disorders of man and animals. Among these are Creutzfeldt-Jakob disease (CJD) in humans and bovine spongiform encephalopathy (BSE) in cattle, with the latter giving rise to the zoonotic appearance of variant CJD (vCJD). One specific characteristic of prion diseases is that the infectious agents appear to consist exclusively of an abnormally folded isoform of the cellular prion protein PrP^{c}, termed PrP^{Sc} [1–3]. PrP^{c} is a sialoglycoprotein expressed mainly in the central nervous system [4]. It is attached to the outer leaflet of the plasma membrane by a glycosyl-phosphatidyl-inositol (GPI) anchor (reviewed in [5]). In a posttranslational process the mainly α-helical PrP^{c} is converted into PrP^{Sc}, which has a high β-sheet content and accumulates within brains of affected individuals [6, 7].

For cellular conversion of PrP^{c} into PrP^{Sc} several premises need to be fulfilled. First, expression of PrP^{c} is absolutely necessary [8]. Second, localization of PrP^{c} at the cell surface [9, 10] and its proper conformation [11, 12] are required. As a GPI-anchored protein, PrP^{c} and also PrP^{Sc} are found in lipid rafts [13, 14], which are membrane microdomains rich in cholesterol and sphingolipids. Due to selective localization of proteins in lipid rafts and spatial proximity, rafts serve as platforms for controlled protein-protein interactions and for initiation of signaling events [15]. For the formation of lipid rafts, free intracellular cholesterol is necessary. The content of free cholesterol within cells is tightly regulated by endogenous synthesis, uptake via low density lipoprotein (LDL) receptors, and the level of esterification, which enables storage of cholesterol in cytoplasmic lipid droplets. Within the central nervous system, neurons downregulate their endogenous cholesterol

synthesis and depend mainly on cholesterol synthesized and released by astrocytes bound to lipoproteins [16]. Upon receptor-mediated endocytosis, cholesterol is released from its transport protein in endosomes and is partially recycled to the plasma membrane, to the trans-Golgi network (TGN), or to the endoplasmic reticulum (ER) [17]. One protein involved in this recycling is NPC-1, a late endosomal/lysosomal transmembrane protein that harbors a putative sterol sensing domain [18]. It appears to be involved in the vesicular transport of LDL-derived cholesterol to the ER and the plasma membrane [19]. Mutations in NPC-1 lead to abrogation of this pathway and to accumulation of free cholesterol and other metabolites such as glycosphingolipids in the late endocytic pathway, resulting in Niemann-Pick type C disease (NPC), a fatal autosomal recessive neurodegenerative disorder [20]. Mechanistically, NPC-1 appears to interact with cholesterol-containing vesicles to mediate their retrograde transport. Mutations within the protein appear to impair fission of NPC-1-positive vesicles from cholesterol-laden organelles leading to accumulation of cholesterol [19].

In prion-infected cells, depletion of cholesterol by inhibition of its synthesis reduces PrP^{Sc} in the neuronal cell lines GT-1 or N2a infected with RML prions [21, 22]. This treatment has been shown to perturb lipid raft formation and can lead to a block of PrP^{c} transport to the plasma membrane [23]. Extraction of membrane cholesterol by methyl-β-cyclodextrin [24], filipin [25], or complexation of membrane cholesterol by amphotericin B [26] also reduced the PrP^{Sc} content of cultured cells. When the signal peptide for GPI anchoring of PrP^{c} is replaced by different transmembrane domains to alter the membrane distribution of PrP^{c} and to prevent its association with lipid rafts, these mutant PrPs were not converted into PrP^{Sc} in persistently prion-infected cells [21, 27], supporting the importance of lipid raft localization for prion conversion. In vivo, the cholesterol synthesis inhibitor simvastatin prolonged incubation times of prion disease in mice [28, 29]; however, this effect is probably due to neuroprotective actions of the drug [29, 30]. Amphotericin B and its less toxic derivative MS-1809 both inhibit prion disease progression although the effect depends on the prion strain used for infection, and the drugs appear to be more effective against BSE prions than scrapie prions [31, 32].

Most of the studies performed on the relationship between cholesterol and PrP^{Sc} generation focused on the impact of an inhibited cholesterol synthesis or of alterations in plasma membrane cholesterol levels, accompanied by perturbations of lipid rafts. However, the role of cholesterol recycling in PrP^{Sc} propagation is only poorly understood. For example, blocking this pathway induces alterations in the subcellular distribution of lipid rafts [33, 34], which could affect PrP^{Sc} biogenesis. Furthermore, cells that accumulate cholesterol, e.g., CHO cells with mutations in the NPC-1 gene or fibroblasts derived from NPC-1 patients, show defects in vesicle transport due to immobilization of rab proteins on membranes enriched in cholesterol [35].

Thus, alterations caused by such conditions might subsequently influence PrP^{Sc} formation in persistently infected cells. Therefore, the aim of our study was to elucidate whether cholesterol accumulation in the late endocytic pathway interferes with cellular prion infection. To achieve cholesterol accumulation, NPC-1 knock-down using small interfering RNA (siRNA) and the compound U18666A, which is commonly used to phenocopy mutations in the NPC-1 gene and which leads to cholesterol accumulation within several hours of treatment [36–38], were used. Under both conditions, PrP^{Sc} accumulation was reduced in prion-infected cells in a dose- and time-dependent manner, due to increased degradation of PrP^{Sc}. Interestingly, rab 9 overexpression partially restored the negative effects of cholesterol accumulation on PrP^{Sc} propagation. Our data provide novel insights into the relationship between cholesterol homeostasis and PrP^{Sc} formation and suggest that recycling of cholesterol and possibly also of PrP^{Sc} is necessary to sustain its persistent propagation in prion-infected neuronal cells.

Materials and methods

Reagents

Proteinase K and Pefabloc proteinase inhibitor were obtained from Roche Diagnostics, (Mannheim, Germany). Immunoblotting was done using the enhanced chemiluminescence blotting technique (ECL plus) from GE Healthcare (Buckinghamshire, UK). The monoclonal anti-PrP antibody (mAb) 4H11 and polyclonal antibody (pAb) A7 have been described [39]. Polyclonal anti-NPC-1 antibody and NPC-1 siRNA were purchased from Abcam (Cambridge, UK) and Santa Cruz (Heidelberg, Germany), respectively. Secondary antibodies for immunofluorescence were Cy2- or Cy3-conjugated immunoglobulins obtained from Dianova (Hamburg, Germany). Poly-L-lysine, bafilomycin A, anti-β-actin antibody, and U18666A were from Sigma (Deisenhofen, Germany). Protein A-Sepharose was obtained from GE Healthcare, sulfo-NHS-biotin was from Pierce (Bonn, Germany). Cell culture media and solutions were obtained from Invitrogen (Karlsruhe, Germany).

Cell culture and treatment of cells

The cell lines 3F4-N2a, stably overexpressing a 3F4-tagged murine PrP, and ScN2a have been described [40]. GT-1 [41] and SN56 were subcloned prior to infection of single

clones with prion strain 22L-infected mouse brain homogenate (ScGT1 and ScSN56, respectively). Cells were kept in Opti-MEM (Invitrogen, Karlsruhe, Germany) containing 10% fetal bovine serum and penicillin/streptomycin. Treatment with U18666A was performed as indicated. Media were changed every other day, and fresh substances were added at each medium change.

Transient transfection of cells with plasmids and siRNA

Transient transfections of ScN2a cells with pEGFP-rab9 and pcDNA3.1 (control) were done using Fugene 6 transfection reagent (Roche, Mannheim, Germany) according to manufacturer's instructions. Treatment with U18666A was started 24 h post transfection. For transfection of ScN2a cells with siRNA, Lipofectamine 2000 (Invitrogen, Karlsruhe, Germany) was used. Twenty nanomoles of NPC-1 or ns siRNA was added for 24 h; after 2 days, lysis of cells and PK digestion were performed.

Detergent solubility assay

Cells were lysed in lysis buffer as described for immunoblot analysis. Postnuclear cell lysates (without PK treatment or following PK (20 μg/ml) digestion) were supplemented with proteinase inhibitors (aprotinin, Pefabloc and PMSF) and N-lauryl sarcosine to 1%, and ultracentrifuged in a Beckman TL-100 table ultracentrifuge for 1 h at 40,000 rpm (100,000 *g*; TLA-45 rotor; 4°C). Supernatant fractions (*S* soluble fraction) were precipitated with five volumes of methanol, pellet fractions (*P* insoluble fraction) were resuspended in 50 μl of TNE and analyzed in immunoblot assays.

PIPLC digestion

For PIPLC treatment, cells were used at about 80% confluency. After 2 washes with PBS, 200 mU of PIPLC (Sigma, Deisenhofen, Germany) were added in 4 ml serum-free DME medium and incubated for 4 h at 37°C. The cells were washed with PBS, lysed as described for immunoblotting, and following methanol precipitation, analyzed by immunoblot.

Surface biotinylation and immunoprecipitation

Cells were treated for 2 days with U18666A (3 μg/ml). After washing the cells twice with PBS, sulfo-NHS-biotin (250 μg/ml in PBS) was added for 10 min on ice. After removal of biotin, cells were chased for 60 min at 37°C (−/+ U18666A) or kept on ice (0 min). Then one plate each of U18666A-treated or mock-treated cells was incubated with trypsin for 10 min on ice; a second plate was left without trypsin treatment. Trypsin digestion was terminated by addition of soybean trypsin inhibitor. All cells were lysed and PrP was immunoprecipitated with pAb A7 as described [42]. Immunoprecipitated PrP was separated by SDS-PAGE followed by immunoblot, and biotinylated PrP was visualized using HRP-streptavidin. Signals of the 60 min time point of three experiments were densitometrically analyzed (ImageQuant TL; GE Healthcare) and evaluated statistically (GraphPad Prism software). Intracellular PrP levels (+ trypsin) were expressed as percentage of total PrP represented by PrP^{c} signals without trypsin digestion.

Flotation assay for detergent-resistant microdomains

For the isolation of detergent-resistant microdomains (DRM) or lipid rafts, 3×10^7 cells were solubilized in 400 μl lysis buffer (NaCl 150 mM, Tris–HCl pH 7.5 25 mM, EDTA 5 mM, and Triton-X 100 1%) and incubated on ice in the cold room for 30 min. The cell lysate was mixed with Nycodenz 70% in TNE (NaCl 150 mM, Tris–HCl pH 7.5 25 mM, EDTA 5 mM) to a final concentration of 35% Nycodenz and loaded into an ultracentrifuge tube. This fraction was overlaid by a discontinuous Nycodenz gradient formed by 200-μl fractions of Nycodenz solutions with concentrations of 25, 22.5, 20, 18, 15, 12, and 8%. After ultracentrifugation (200,000 *g*, 4 h, 4°C, Beckmann TLS55 rotor), 200-μl fractions were collected from the top to the bottom of the gradient and precipitated with five volumes of methanol. After centrifugation for 30 min at 3,500 rpm, the pellets were resuspended in TNE and an aliquot of each fraction was analyzed by immunoblot. For identification of lipid rafts, an aliquot of each fraction was subjected to dot blot analysis using HRP-conjugated cholera toxin B (Ctx B). Ctx B binds to the glycosphingolipid GM-1, which is a marker for lipid rafts.

Indirect immunofluorescence assay and confocal microscopy

Cells were seeded on poly-L-Lysine-coated glass cover slips (Marienfeld, Germany) at low density 1–3 days prior to staining. Cells were washed twice in cold PBS and fixed in 4% paraformaldehyde for 30 min at room temperature. After sequential treatments with NH_4Cl (50 mM in 20 mM glycine), Triton-X 100 (0.3%), and gelatin (0.2%) for 10 min each at room temperature, primary antibodies were added at a 1:100 dilution in PBS and incubated for 30 min at room temperature. After three washes in PBS, Cy2- or Cy3-conjugated secondary antisera (1:100 dilution in PBS) were applied for 30 min at room temperature. Slides were mounted in anti-fading solution (5% propyl gallate in 70%

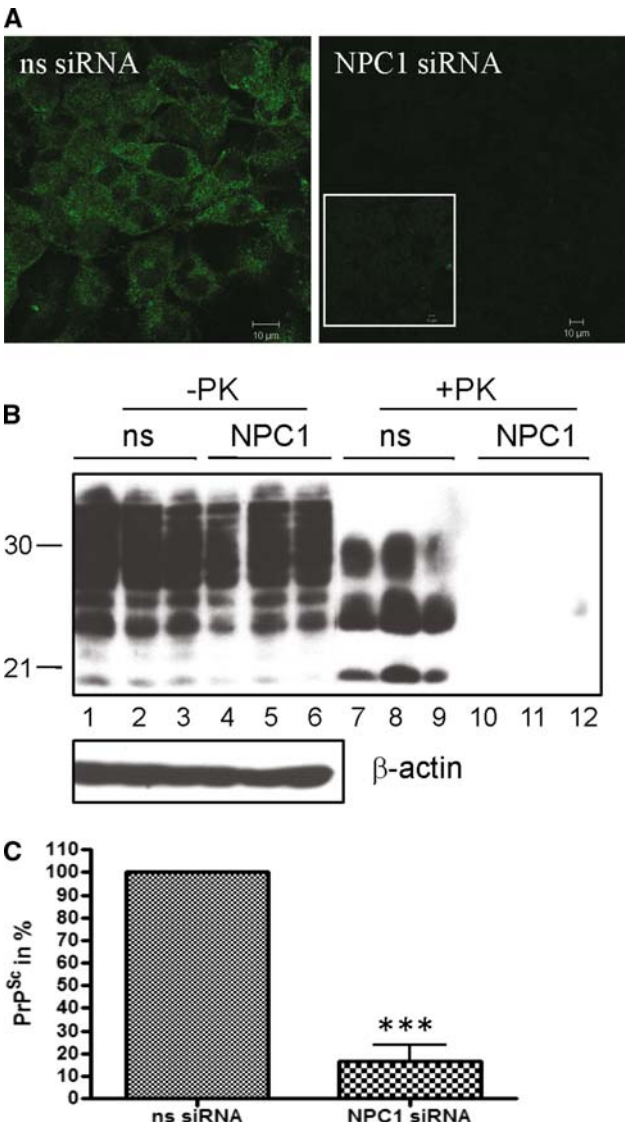

Fig. 1 Knock-down of NPC-1 drastically reduces PrP^{Sc}. **a** ScN2a cells were transiently transfected with non-silencing (ns) siRNA or siRNA targeting NPC-1 mRNA. Two days post transfection, cells were stained with anti-NPC-1 antibody and Cy2-conjugated anti-rabbit IgG. Staining was visualized by confocal laser scanning microscopy, using identical immunofluorescence settings. The *inset* shows the image of cells transfected with NPC-1 siRNA excited with higher voltage to demonstrate presence of cells. **b** Transient transfections of ScN2a cells were performed in triplicate with ns siRNA or NPC-1 siRNA. Two days after transfection, cells were lysed and lysates were treated with (+*PK*) or without (−*PK*) PK. SDS-PAGE and immunoblot were performed, and for detection of PrP, monoclonal antibody 4H11 was used. To confirm equal loading, the immunoblot was reprobed with an antibody against β-actin (*lower panel*; -PK). **c** Quantification and statistical analysis of the effect of NPC-1 knock-down on PrP^{Sc} propagation. ScN2a cells transfected transiently with ns or NPC-1 siRNA were lysed 2 days post transfection. The amount of PrP^{Sc} upon PK digestion detected by immunoblot was densitometrically evaluated. The value for PrP^{Sc} in ns siRNA transfected cells was set to 100%; the amount in NPC-1 siRNA transfected cells was expressed as a percentage thereof. For statistical analysis, results of four independent experiments were used. Two out of four experiments were performed in duplicate and triplicate, respectively, and of these, the average percentage of PrP^{Sc} in relation to the control (ns siRNA) was used for statistical analysis (*** $P < 0.005$; *t*-test)

glycerol; 100 mM Tris–HCl, pH 9.0) and kept dry at −20°C. Confocal laser scanning microscopy was done using a Zeiss (Göttingen, Germany) LSM510 confocal microscope.

Results

Inhibition of cholesterol recycling reduces PrP^{Sc} in persistently prion-infected cultured cells

For many years it has been well established that cellular cholesterol metabolism plays an important role for PrP^{Sc} propagation. Inhibition of HMG-CoA reductase or other enzymes involved in cholesterol synthesis or application of compounds that bind or extract free membrane-bound cholesterol such as amphotericin B can significantly reduce cellular PrP^{Sc} conversion or even prolong incubation time of prion disease in animal models. However, the impact of cholesterol membrane distribution and trafficking has not been investigated in detail so far.

Following endocytosis of LDL-cholesterol via the LDL receptor and its dissociation from LDL, a large amount of free cholesterol is recycled back to the plasma membrane. One protein implicated in this transport is NPC-1. Therefore, one way to inhibit cholesterol transport in cultured cells is to knock-down NPC-1 expression by transfection of cells with siRNA. In line with this, we transiently transfected RML-infected N2a cells (ScN2a) with siRNA targeting NPC-1 mRNA or non-silencing (ns) siRNA (Fig. 1). The efficiency of the knock-down was analyzed by immunofluorescence assay using an anti-NPC-1 antibody (Fig. 1a). In cells transfected with ns siRNA, a strong vesicular staining was observed (left image), whereas no specific fluorescence signal was detectable in cells transfected with NPC-1 siRNA under identical immunofluorescence conditions (right image). The inset shows the image excited with higher voltage and here, in single cells, residual fluorescence signals were detectable. This proves that NPC-1 siRNA very efficiently silenced the target gene. Similar results were obtained by immunoblot assay using an anti-NPC-1 antibody (Suppl. Fig. 1a).

Next, the effect of NPC-1 knock-down on cellular PrP^{Sc} content was analyzed. Again, ScN2a cells were transiently transfected with ns or NPC-1 siRNA (Fig. 1b). To support

the significance of data obtained here, the experiment was performed several times, including triplicate assay. Two days post transfection, cells were lysed, an aliquot was digested with PK, and all lysates were analyzed by immunoblot. In samples without PK digestion (lanes 1–6) no major differences in total PrP signals were detectable. In contrast, PK-treated samples from cells transfected with ns siRNA harbored high amounts of PrP^{Sc} (lanes 7–9; N-terminally trimmed PrP; un-, mono-, and di-glycosylated forms), whereas in NPC-1 siRNA-transfected cells, PrP^{Sc} was not detectable under these conditions. Reprobing the membrane with anti-β-actin antibody confirmed equal loading. Statistical analysis of the results of four independent experiments revealed a highly significant reduction in PrP^{Sc} levels in cells transfected with NPC-1 siRNA (Fig. 1c). However, if transiently transfected cells were lysed 3 or 4 days post transfection with siRNAs, PrP^{Sc} signals in NPC-1 siRNA-transfected cells increased again at day 3 and were almost equal to the signal in control cells at day 4 after transfection (Suppl. Fig. 1b). This could be explained by the only transient knock-down of NPC-1 expression, which in parallel with the re-appearance of PrP^{Sc}, increased at days 3 and 4 post transfection as demonstrated by immunoblot analysis (Suppl. Fig. 1a).

In summary, efficient knock-down of NPC-1 by siRNA leads to a significant transient reduction of PrP^{Sc} in ScN2a cells.

U18666A treatment reduces PrP^{Sc} in persistently infected cells but does not inhibit primary infection

Similar to NPC-1 knock-down, cholesterol accumulation in late endosomes/lysosomes can be induced by treatment with the negatively charged amine U18666A. Unfortunately, the targets of U18666A have not been characterized so far, and therefore the exact mechanism of action of this drug is unknown [34]. It was suggested that the compound acts directly on the NPC-1 pathway to induce lysosomal accumulation of cholesterol [37], and, in addition, inhibits an enzyme of the cholesterol synthesis pathway [43]. Since cholesterol accumulation induced by U18666A is well documented and the drug is commonly used to induce an NPC phenotype in cultured cells [36–38], we employed the compound in our further experiments. First, we investigated whether the effects of NPC-1 knock-down on cellular PrP^{Sc} content are reproduced by U18666A treatment. ScN2a cells were treated for 3 days with increasing concentrations of U18666A (0, 1, 3, or 5 μg/ml, a range which is frequently used to induce cholesterol storage within several hours) [19, 34, 37]. Samples with or without PK digestion were analyzed by immunoblot for PrP signals (Fig. 2a). In untreated cells, a strong PrP^{Sc} signal was visible (lane 2), which was significantly reduced by 1 μg/ml of U18666A (lane 4) and undetectable by 3 (lane 6) or 5 μg/ml (lane 8) of the drug. The amount of PrP^{c} was not significantly influenced by the treatment (lanes — PK, total PrP). In addition, ScN2a cells were treated with 0 or 3 μg/ml U18666A for 3 and 7 days. To enable comparison of signals in treated and untreated cells, for each time point one control culture was lysed in parallel. Aliquots with or without PK treatment were subjected to immunoblot (Fig. 2b). Again, PrP^{Sc} was reduced to undetectable levels, whereas in untreated control cells, a clear PrP^{Sc} signal was visible (lanes + PK). The increase in PrP^{Sc} signals between day 3 and day 7 in control cells is indicative for accumulation of PrP^{Sc} during cultivation. PrP^{c} levels were not altered by the treatment (lanes — PK). A similar reduction of PrP^{Sc} by U18666A treatment was observed in N2a cells infected with prion strain 22L (data not shown).

In order to verify that the observed effects on PrP^{Sc} generation were not specific for ScN2a cells, two further prion-infected cell lines were tested, namely ScGT-1 (Suppl. Fig. 2a) and ScSN56 (Suppl. Fig. 2b) cells. These cells were treated with lower concentrations of the drug for 3 (ScSN56) or 8 days (ScGT-1). In these cell lines, the anti-prion effect of U18666A could be confirmed. Of note, toxicity of the compound was excluded in all three cell lines by XTT assay for the concentrations and durations of treatment chosen for this study (data not shown).

The next question was whether the presence of U18666A during primary prion infection can inhibit the establishment of persistent infection (Fig. 2c). 3F4-N2a cells susceptible to infection were left untreated or were pre-treated for 4 h with U18666A (3 μg/ml). Subsequently, brain homogenates from terminally sick mice infected with RML or 22L prions were added for 24 h. During infection, cells were either left untreated (−) or U18666A was added during the 24 h of brain homogenate incubation (+) or the pre-treatment was continued for the infection period (+4; 28 h treatment in total). After removal of brain homogenates and drug, cells were further passaged. Passage 3 was lysed and a solubility assay of cell lysates with or without PK digestion was performed. Insoluble fractions of samples + PK (P/+ PK; lanes 1–6) harboring PrP^{Sc} and supernatant fractions of samples — PK (S/–PK; lanes 7–12) containing soluble PrP^{c} were subjected to immunoblot analysis. To selectively detect newly converted PrP^{Sc}, mAb 3F4 was used. Independent of treatment and prion strain, all cell cultures harbored high amounts of 3F4-positive PrP^{Sc}, indicative of primary prion infection.

In summary, similar to the NPC-1 knock-down, treatment with U18666A reduces PrP^{Sc} content in persistently infected ScN2a, ScGT-1, and ScSN56 cells. However, primary infection of 3F4-N2a cells was not inhibited by the drug.

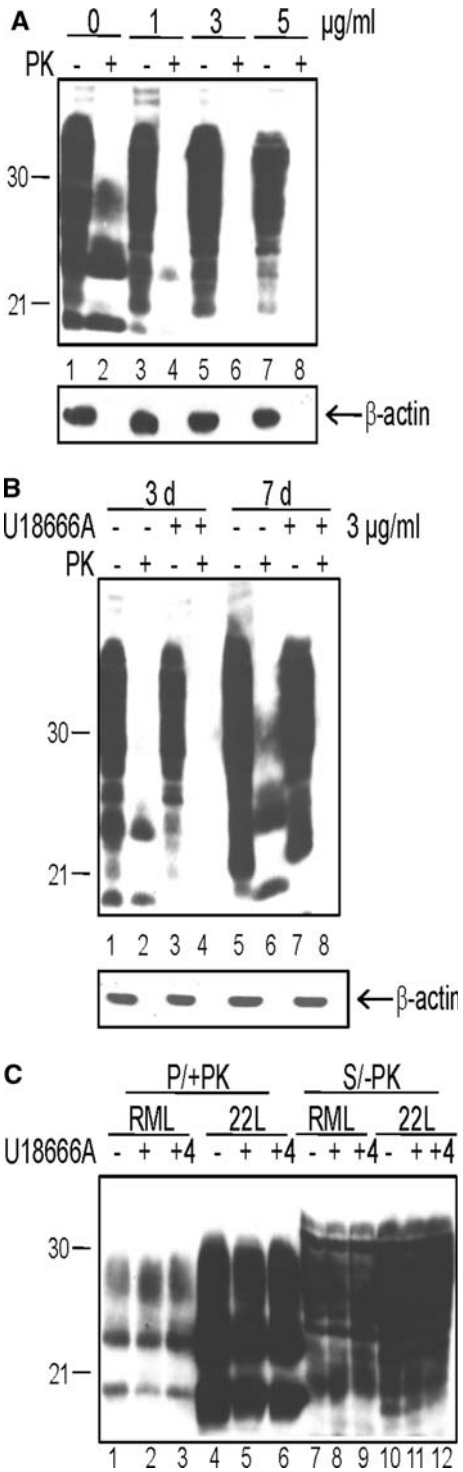

Fig. 2 Dose- and time-dependent reduction of PrP^{Sc} in persistently infected cells, but no inhibition of primary infection upon chemical induction of lysosomal cholesterol accumulation. **a** ScN2a cells were treated for 3 days with various concentrations (0, 1, 3, or 5 µg/ml) of U18666A as indicated. Cells were lysed, digested with PK (+*PK*) or not (−*PK*), and proteins were analyzed by immunoblot. Mab 4H11 was used for detection of PrP-specific bands. The immunoblot was dehybridized and incubated with an anti-*β*-actin mAb to control for equal loading (*lower panel*). **b** Treatment of ScN2a cells with U18666A (3 µg/ml) was performed for 3 and 7 days in parallel to mock treatment. At the different time points, U18666A-treated and mock-treated cells were lysed. Lysates were digested with PK (+*PK*) or not (−*PK*) and were subjected to immunoblot analysis using mAb 4H11. Equal loading of lysates of the different time points was confirmed by reprobing the membrane with anti-*β*-actin mAb (*lower panel*). **c** 3F4-N2a cells were left untreated or were pretreated for 4 h with U18666A (3 µg/ml) prior to prion infection. For prion infection, brain homogenates (1%) from RML- or 22L-infected terminally sick mice were added for 24 h to the culture medium. Cells that had not been pretreated were infected either in the presence (+) or absence (−) of U18666A for 24 h. For pretreated cells, the U18666A treatment was continued for the time period of infection (+4; 28 h treatment in total). After 24 h, brain homogenates and U18666A were removed, cells were washed and passaged three times 1:10. Passage 3 was lysed, lysates were treated with PK (+*PK*) or left untreated (−*PK*) and were then subjected to a solubility assay. Pellet fractions of samples + PK (*P*/+*PK*) and supernatant fractions of samples −PK (*S*/−*PK*) were analyzed by immunoblot with mAb 3F4, which selectively detects newly generated 3F4-PrP^{Sc} in the pellet fractions (P/+PK) and 3F4-PrP^{c} in the supernatant (S/−PK)

PrP^{c} plasma membrane turnover and lipid raft association are not perturbed by U18666A

Frequently, the mode of action of PrP^{Sc}-reducing compounds in cell culture is an altered localization or turnover of PrP^{c} that does not necessarily implicate an altered signal for total PrP^{c} content as detected by immunoblot [44]. In particular, perturbation of cellular cholesterol metabolism might influence PrP^{c} transport to the plasma membrane or its localization in lipid rafts.

To exclude such effects, the subcellular localization of PrP^{c} in U18666A-treated cells was investigated. N2a cells were treated for 3 days with U18666A. Subsequently, PIPLC digestion was performed, which releases GPI-anchored proteins from the cell surface. In both U18666A-treated and untreated cells, PrP^{c} was undetectable in cell lysates after PIPLC treatment (Fig. 3a; lanes 2 and 4), indicating that PrP^{c} plasma membrane localization was not impaired by U18666A. This was confirmed by immunofluorescence assay performed with U18666A-treated or untreated N2a cells (Fig. 3b). Again, under both conditions PrP^{c} was clearly detectable at the cell surface.

Next, we tested whether the turnover of PrP^{c} at the cell surface was changed by U18666A treatment. N2a cells were treated with U18666A or were left untreated for control, and biotinylation of cell surface proteins was performed. The amounts of total (−trypsin) and internalized (+trypsin) PrP^{c} were analyzed by immunoblot. Figure 3c shows a representative immunoblot of several independent experiments. At 0 min, almost all PrP^{c} could be released by trypsin indicating that the majority of PrP^{c} was located at the cell surface and only small amounts were already internalized (lanes 2 and 4). After 60 min, in control cells slightly less PrP^{c} than in U18666A-treated cells was accessible for trypsin, indicating that more PrP^{c}

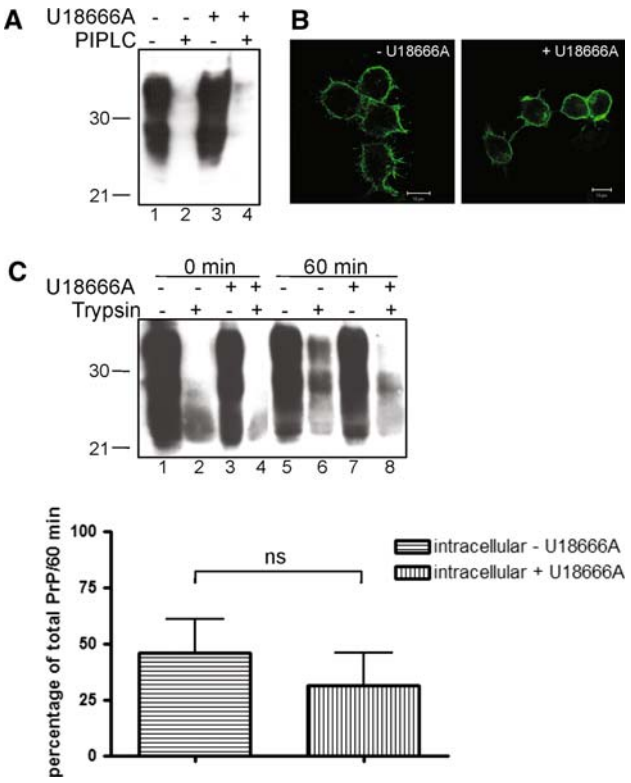

Fig. 3 No changes in membrane localization and turn-over of PrP^c in U18666A treated N2a cells. **a** N2a cells were treated for 3 days with U18666A (3 μg/ml) or left untreated as indicated. For release of PrP^c by PIPLC (*left panel*), cells were incubated for 4 h with or without the enzyme. Treatment with U18666A was continued during PIPLC digestion. Then cells were lysed and lysates were subjected to immunoblot analysis using mAb 4H11for detection of PrP specific bands. **b** N2a cells with or without U18666A treatment for 3 days were fixed, permeabilized, and stained in indirect immunofluorescence with anti-PrP mAb 4H11 and Cy2-conjugated anti-mouse IgG. **c** Biotinylation of N2a cells treated for 2 days with or without U18666A was performed and cultures were chased at 37°C in culture medium −/+U18666A for 60 min or were processed immediately. After 0 or 60 min chase, one culture dish each of treated or untreated cells was incubated with trypsin. PrP from cell lysates was immunoprecipitated using pAb A7, subjected to immunoblot, and detected by incubation with horseradish peroxidase (HRP)-conjugated streptavidin. A representative immunoblot of three independent experiments is shown. PrP^c signals of the 60 min time point with (internalized PrP^c) or without (total PrP^c) trypsin digestion were densitometrically analyzed. The amount of internalized PrP^c was expressed as a percentage of total PrP^c. The *lower panel* depicts statistical evaluation of the difference between internalized PrP^c in mock-treated or U18666A-treated cells using Student's *t*-test (*ns* not significant; *P*-value >0.05; *bars* indicate standard error)

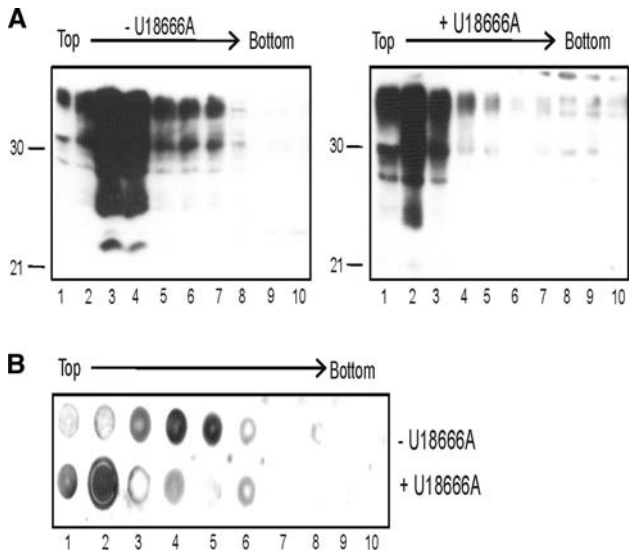

Fig. 4 Lipid raft association of PrP^c is not altered in U18666A-treated cells. **a** N2a cells were treated for 3 days with U18666A (*right panel*) or left untreated (*left panel*) and were subjected to a flotation assay. Ten fractions from the top to the bottom of the centrifuge tube were collected and analyzed by immunoblot with mAb 4H11. **b** Aliquots of gradient fractions were spotted on a nitrocellulose membrane and GM1 was detected by incubation of the membrane with HRP-conjugated cholera toxin subunit B (CtxB)

was internalized without treatment (lane 6 vs. lane 8). Densitometric analysis revealed that in control cells ~55% of total PrP^c was internalized, whereas in U18666A-treated cells only ~35% was found within the cells. However, this difference was not statistically significant (Fig. 3c).

Alterations in cholesterol metabolism may implicate that lipid raft assembly or localization of proteins in these membrane domains is disturbed. To verify this, detergent-resistant microdomains were isolated, and flotation assays were performed with U18666A-treated or untreated N2a cells (Fig. 4). Fractions of the gradients were collected and analyzed by immunoblot (Fig. 4a). Without treatment (−U18666A), the majority of PrP^c partitioned in fractions 3 and 4, which correlates with the presence of the lipid raft marker GM1 in these fractions (Fig. 4b). In treated cells (+U18666A), localization of PrP^c signals again correlated with GM1 signals. However, peak levels were shifted from fractions 3 and 4 in untreated cells to fraction 2.

These data indicate that U18666A treatment has no major detectable effects on PrP^c endocytosis and/or recycling. Despite drug treatment, it is localized within detergent-resistant membrane domains.

No influence of U18666A treatment on cellular *de novo* generation of PrP^{Sc}

Our data obtained so far demonstrate that alterations in PrP^c plasma membrane localization are probably not responsible for the observed reduction of PrP^{Sc} levels in ScN2a cells upon U18666A treatment. Since cholesterol accumulation upon NPC-1 knock-down or U18666A treatment occurs in late endosomes/lysosomes, cell biological effects induced by the treatments are likely exerted in the late endocytic pathway.

Consequently, we analyzed whether—under combined bafilomycin A (Baf A) and U18666A treatment—PrP^{Sc} can be detected in ScN2a cells. Bafilomycin A prevents protein transport from early to late endosomes by inhibiting acidification and maturation of those vesicles. Thereby, the degradation of proteins is prevented. The combined treatment might give hints to whether U18666A prevents synthesis of PrP^{Sc} or rather induces its degradation. ScN2a cells were treated for 24 h with U18666A or left untreated. Then cells were lysed and lysates were digested with PK. In parallel, in ScN2a cultures, U18666A treatment was continued for 2 days, either in combination with Baf A or not. Untreated cells and cells treated only with Baf A served as controls. PK-treated lysates were analyzed in immunoblot (Fig. 5 upper panel; duplicate assay). After 24 h (lanes 1–4), PrP^{Sc} was detectable in controls but not in U18666A-treated cells. These PrP^{Sc} signals served as baseline levels for comparison with PrP^{Sc} signal intensities after continued cultivation either without treatment (lanes 5 and 6), with U18666A (lanes 7 an 8) or Baf A (lanes 9 and 10) alone, or with a combination of U18666A and Baf A (lanes 11 and 12). Upon continued culture (day 3), in control cells without treatment a strong PrP^{Sc} signal was visible which was clearly higher than that at day 1 (lanes 5 and 6 vs. lanes 1 and 2). As expected, in U18666A treated cells (lanes 7 and 8) the signal again was lower than in untreated cells. However, Baf A treatment led to a strong increase of PrP^{Sc} signals in both controls (lanes 9 and 10) and U18666A-treated (lanes 11 and 12) cells due to impaired degradation of PrP^{Sc} between day 1 and day 3. This indicates that despite cholesterol accumulation in endosomal vesicles, PrP^{Sc} can be formed. In case the Baf A treatment were to only inhibit degradation of pre-existing PrP^{Sc}, the signal after 3 days would not exceed the initial signal after 1 day treatment (compare lanes 3 and 4 to lanes 11 and 12). Analysis of corresponding samples without PK digestion (Fig. 5 lower panel) with anti-β-actin and anti-PrP antibodies served as control for comparable loading at the different time points. The increase in PrP^{c} and PrP^{Sc} signals between day 1 and day 3 is due to higher cell numbers and accumulation of PrP^{Sc} which is newly formed between day 1 and day 3. A further hint for ongoing generation of PrP^{Sc} in U18666A-treated cells was provided by metabolic labeling of ScN2a cells followed by immunoprecipitation of PrP^{Sc} (data not shown).

In summary, these data demonstrate that PrP^{Sc} can be formed in U18666A-treated cells and that the treatment rather enhances degradation of PrP^{Sc}.

Rab 9 overexpression partially restores PrP^{Sc} contents in U18666A-treated cells

It has been demonstrated previously that cholesterol accumulation in late endosomal/lysosomal compartments

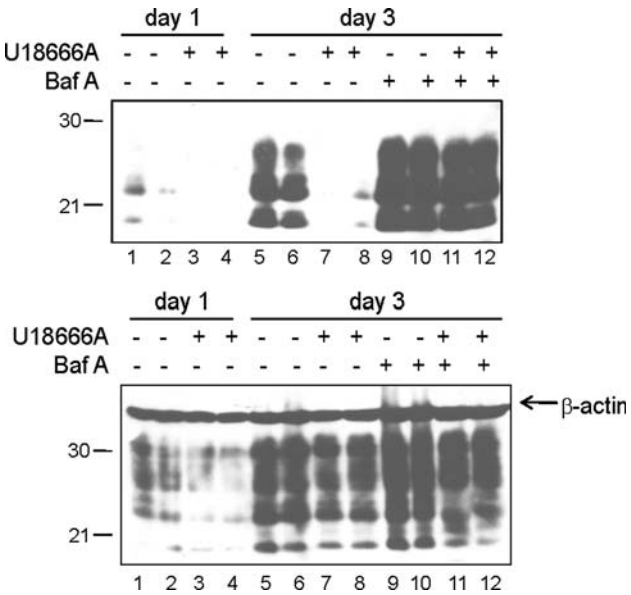

Fig. 5 U18666A treatment increases PrP^{Sc} degradation. *Upper panel* ScN2a cells were treated for 1 day with U18666A (3 μg/ml) or were left untreated. Cells were either lysed after 1 day and lysates were treated with PK (lanes 1–4) or were incubated for further 2 days (day 3; lanes 5–12) with or without U18666A in presence or absence of bafilomycin A (10 nM). Then cells were lysed and subjected to PK digestion. All samples were separated by SDS-PAGE followed by immunoblot. For detection of PrP, mAb 4H11 was used. The experiment was performed in duplicate. *Lower panel* Samples without PK digestion were analyzed by immunoblot for total PrP using mAb 4H11 and for β-actin levels (*arrow*) for control of equal loading

can be attenuated by overexpression of rab 9 [45], implicating that this might alleviate the negative influence of U18666A on PrP^{Sc} propagation. To verify this hypothesis, an EGFP-rab 9 fusion protein was transiently overexpressed in U18666A-treated and untreated ScN2a cells. FACS analysis of cells expressing EGFP-rab 9 revealed a transfection efficiency of ~70% (data not shown). As controls, ScN2a cells were transfected with empty vector. One day post transfection, U18666A was added for 2 days. Samples of PK-digested lysates were subjected to immunoblot analysis. Figure 6 shows a representative experiment performed in duplicate. Control cells (pcDNA3.1) harbored high amounts of PrP^{Sc}, which were diminished by U18666A treatment (left panel). Surprisingly, rab 9 overexpression appeared to reduce PrP^{Sc} levels when compared to cells transfected with empty vector even without U18666A treatment (middle panel). However, the difference in PrP^{Sc} signals between untreated and treated cells overexpressing EGFP-rab 9 (right panel; the inlet depicts EGFP-rab 9 overexpression) appeared to be less pronounced than the one observed between mock-transfected controls with or without U18666A treatment (left panel). To illustrate this, quantification of five independent experiments was done for statistical analysis (Fig. 6; lower

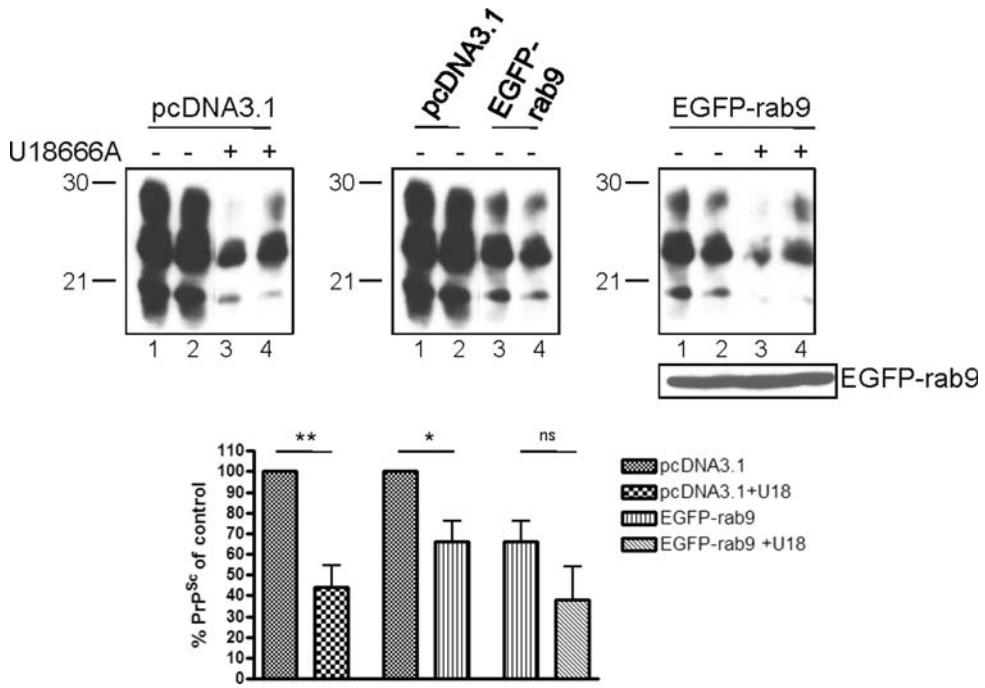

Fig. 6 Rab 9 overexpression impairs PrP^{Sc} propagation but partially rescues the interference induced by cholesterol accumulation. ScN2a cells were transiently transfected with pEGFP-rab 9 or with pcDNA3.1 as a control. Following transfection, treatment with U18666A (3 μg/ml) was performed for 2 days. Then cells were lysed, aliquots were digested with PK, and samples were analyzed by immunoblot using mAb 4H11. A representative duplicate experiment is shown (*upper panel*). To enable better comparison, samples analyzed by one immunoblot were opposed to each other. Expression of EGFP-rab 9 was detected using a polyclonal anti-GFP antibody. PrP^{Sc} signals of five independent experiments were evaluated densitometrically (ImageQuant TL), and statistical analysis was performed (*lower panel*, *ns* not significant; $*P < 0.05$, $**P < 0.005$; *bars* indicate standard error). The signal intensity of untreated mock-transfected controls was set as 100%, and all other values are expressed as a percentage of this value

panel). Both the differences in PrP^{Sc} signals between control cells with U18666A ($P < 0.005$) and between control and rab 9-expressing cells ($P < 0.05$) were statistically significant. In contrast, the signal reduction between rab 9-overexpressing cells treated with U18666A compared to nontreated cells was not significant ($P = 0.183$).

This indicates that although rab 9 overexpression reduces PrP^{Sc} in ScN2a cells, it can attenuate the reduction of PrP^{Sc} content in ScN2a cells induced by cholesterol accumulation in the late endocytic pathway.

Discussion

Cholesterol is an important constituent of biological membranes and is concentrated in lipid rafts together with sphingolipids. Depletion of cholesterol impairs cellular prion conversion, and the study presented here was intended to investigate the impact of cholesterol accumulation in late endosomes on PrP^{Sc} propagation in persistently prion-infected cells and on primary prion infection.

LDL-cholesterol, which is internalized via the LDL-receptor, dissociates in endosomes, and both cholesterol and the LDL-receptor recycle back to the plasma membrane. Two proteins implicated in cholesterol recycling are NPC-1 and NPC-2. Loss-of-function mutations—mainly in the NPC-1, but also in the NPC-2 gene—are associated with Niemann-Pick type C disease (NPC), a neurodegenerative disorder characterized by excessive cholesterol accumulation in late endosomes and lysosomes [45, 46]. In ScN2a cells we found that knock-down of NPC-1 led to a drastic loss of PrP^{Sc}. Similar effects, also in 22L prion-infected N2a cells (data not shown), ScGT-1, and ScSN56 cells were obtained by treatment with the compound U18666A. This is in agreement with previous findings [47, 48], however, the drug appears not to be effective in a mouse model of prion disease [48]. In both studies, significantly lower concentrations of the drug were used to determine the IC_{50} value over 4 days of treatment, a factor which is critical if a drug will be applied in bioassays [47, 48]. In contrast, our main intention was to induce cholesterol accumulation within a short time frame (16 h to 2 days). Therefore, we applied higher concentrations of the drug as described in previous publications [19, 34, 37] which were not toxic to the cells under our experimental conditions to achieve the NPC phenotype. However, U18666A treatment, which phenocopies NPC, does not exclusively inhibit cholesterol recycling within the cell but also to some extent the endogenous cholesterol synthesis

[43]. In contrast to the above mentioned studies [47, 48], our data obtained with siRNA targeting NPC-1 mRNA clearly demonstrate that indeed cholesterol accumulation can cause reduction of PrP^{Sc} in ScN2a cells. Interestingly, primary infection of N2a cells with RML or 22L prions was not inhibited by U18666A. This indicates that initial conversion of PrP^{c} to PrP^{Sc} might occur even under conditions of cholesterol accumulation. However, this initial conversion rate appeared to be insufficient for establishing persistent prion infection when U18666A treatment was continued after removal of brain homogenates (data not shown).

Our results on PrP^{c} localization and trafficking support the assumption that formation of PrP^{Sc} can occur during U18666A treatment. PrP^{c} is located at the cell surface, which is one prerequisite for conversion into PrP^{Sc}, and its recycling is at least not statistically significantly altered. PrP^{c} is still found in lipid rafts, in contrast to what has been suggested previously [47]. The finding that lipid raft formation is not perturbed by U18666A treatment is supported by studies demonstrating that lipid rafts are stabilized in late endosomes in U18666A-treated cells [34] or even accumulate in cells expressing mutated NPC-1 [33]. It is interesting to note that a shift of the raft marker protein caveolin-1 towards lighter fractions of a flotation gradient, which we observed for GM-1 and PrP^{c} in U18666A-treated cells, was induced by infection of a fibroblast cell line with a murine parvovirus [49]. These alterations led to an increased uptake of PrP^{Sc} compared to controls without changing its subcellular distribution [49]. The observation that trafficking of exogenously added PrP^{Sc} is not altered under such conditions supports the plausibility of our finding that despite slight alterations of lipid rafts induced by U18666A treatment, primary infections of N2a cells can be established.

Compounds targeting cholesterol homeostasis previously found to be active against PrP^{Sc} formation in cell culture mainly affected the pool of plasma membrane cholesterol and/or lipid raft formation [20, 22, 24–26]. In contrast, by inducing a NPC phenotype in cultured cells, alterations are expected to occur mainly in late endosomal or lysosomal compartments. That perturbations of PrP^{Sc} propagation are indeed occurring in the late endosomal/lysosomal system is shown by our experiments with co-treatment of cells with U18666A and bafilomycin A. Bafilomycin A inhibits protein degradation, since early to late endosome maturation is impaired due to perturbation of endosomal acidification. However, recycling of early endosomes and their cargo proteins to the plasma membrane is still possible [50]. Upon combined treatment with U18666A and Baf A, which inhibits lysosomal degradation, between day 1 and 3 PrP^{Sc} signals increased (Fig. 5a; lanes 3 and 4 vs. lanes 11 and 12). This demonstrates that, in principle, PrP^{Sc} can be generated during U18666A treatment, but that increased degradation inhibits its accumulation. This is feasible since RML PrP^{Sc} in infected cells might propagate in early endosomes or at the plasma membrane [51], both pathways that are not impaired by Baf A. To elucidate whether recycling from early endosomes to the plasma membrane is important for PrP^{Sc} propagation requires further experiments and is beyond the scope of this study. However, PrP^{Sc} formation is increased in RML-infected N2a cells overexpressing a transdominant negative rab4 mutant [52]; therefore this pathway seems to be dispensable for PrP^{Sc} propagation.

Overall, our data suggest that upon U18666A-induced cholesterol accumulation in the late endosomal/lysosomal compartment degradation of PrP^{Sc} is accelerated. Indeed, the drug can stimulate cellular autophagy [53], a pathway that contributes to the degradation of misfolded protein, e.g., of huntingtin aggregates associated with Huntington's disease [54]. Interestingly, two novel studies demonstrate that induction of autophagy can stimulate the degradation of PrP^{Sc} in prion-infected cells [55, 56]. In NPC−/− mice levels and activity of cathepsin D and B are increased [57]. PrP^{Sc} accumulates in late endosomes [58] and lysosomes [59], where it can be degraded, although it has a rather long half-life of more than 24 h [39, 60]. In particular, lysosomal cystein proteases such as cathepsin B and L are capable of degrading PrP^{Sc} [61, 62], and induction of their activity by inducing a NPC phenotype could also account for improved degradation of PrP^{Sc}.

Impairment of cholesterol transport by NPC-1 knockdown is accompanied by disturbances in vesicle trafficking due to immobilization of rab GTPases [45, 63], which regulate vesicle trafficking and docking to their specific target organelle membranes [64]. In NPC−/− fibroblasts or U18666A-treated cells accumulation of cholesterol in late endosomes can be alleviated by overexpression of rab 9, which increases delivery of cholesterol-laden vesicles and their cargo to the Golgi/TGN and thereby induces redistribution of cholesterol [45, 65]. In ScN2a cells treated with U18666A, we observed that rab 9 overexpression partially rescued PrP^{Sc} propagation. This indicates that cholesterol and/or vesicle recycling to the TGN is necessary for PrP^{Sc} propagation. Furthermore, PrP^{Sc} located within late endosomes might be transported via rab 9-positive vesicles to the Golgi/TGN. Thereby, a certain escape from degradation could be achieved, explaining the partial rescue of the negative U18666A effects. Surprisingly, we found that rab 9 overexpression alone significantly impaired PrP^{Sc} propagation. This apparently contradictory finding might be comparable to the relation between amyloid β-peptide ($A\beta$) production and expression levels of the sorting protein-related receptor sorLA. Upon overexpression of this protein, redistribution of amyloid precursor protein (APP) to the Golgi complex is induced, thereby protecting APP from processing to $A\beta$ [66]. For PrP^{Sc}, a similar balance between

new formation and residence time in certain compartments might exist that could explain, on the one hand, the positive effects in U18666A-treated cells, and, on the other hand, the negative effects of rab 9 overexpression in untreated cells on PrP^{Sc} propagation.

Altogether, our study demonstrates that accumulation of cholesterol in the late endocytic pathway is deleterious for PrP^{Sc} propagation in cultured cells. Rather than perturbation of lipid raft association, we suggest that an increased degradation of PrP^{Sc} is responsible for this effect.

Acknowledgments We are grateful to Dr. D. Marks and Dr. R. Pagano, Mayo Clinic and Foundation, Rochester, MN, USA, for providing the EGFP-rab 9 construct, and to Prof. M. Groschup (Friedrich-Löffler-Institut, Isle of Riems, Germany) for providing prion-infected mouse brains. This work was supported by the German Research Foundation DFG (grant VO1277 and SFB-596 projects A8 and B14), the Alberta Prion Research Institute, Alberta, Canada, and was performed within the framework of European Union FP6 Network of Excellence 'Neuroprion'.

Reference

1. Prusiner SB (1998) Prions. Proc Natl Acad Sci USA 95:13363–13383
2. Weissmann C, Enari M, Klohn PC, Rossi D, Flechsig E (2002) Transmission of prions. J Infect Dis 186(Suppl 2):S157–S165
3. Aguzzi A, Polymenidou M (2004) Mammalian prion biology: one century of evolving concepts. Cell 116:313–327
4. Kretzschmar HA, Prusiner SB, Stowring LE, Dearmond SJ (1986) Scrapie prion proteins are synthesized in neurons. Am J Pathol 122:1–5
5. Nunziante M, Gilch S, Schatzl HM (2003) Prion diseases: from molecular biology to intervention strategies. Chembiochem 4:1268–1284
6. Prusiner SB, Scott M, Foster D, Pan KM, Groth D, Mirenda C, Torchia M, Yang SL, Serban D, Carlson GA (1990) Transgenetic studies implicate interactions between homologous PrP isoforms in scrapie prion replication. Cell 63:673–686
7. Come JH, Fraser PE, Lansbury PT Jr (1993) A kinetic model for amyloid formation in the prion diseases: importance of seeding. Proc Natl Acad Sci USA 90:5959–5963
8. Bueler H, Aguzzi A, Sailer A, Greiner RA, Autenried P, Aguet M, Weissmann C (1993) Mice devoid of PrP are resistant to scrapie. Cell 73:1339–1347
9. Taraboulos A, Raeber AJ, Borchelt DR, Serban D, Prusiner SB (1992) Synthesis and trafficking of prion proteins in cultured cells. Mol Biol Cell 3:851–863
10. Caughey B, Raymond GJ (1991) The scrapie-associated form of PrP is made from a cell surface precursor that is both protease- and phospholipase-sensitive. J Biol Chem 266:18217–18223
11. Gilch S, Nunziante M, Ertmer A, Wopfner F, Laszlo L, Schatzl HM (2004) Recognition of lumenal prion protein aggregates by post-ER quality control mechanisms is mediated by the preoctarepeat region of PrP. Traffic 5:300–313
12. Nunziante M, Kehler C, Maas E, Kassack MU, Groschup M, Schatzl HM (2005) Charged bipolar suramin derivatives induce aggregation of the prion protein at the cell surface and inhibit PrPSc replication. J Cell Sci 118:4959–4973
13. Vey M, Pilkuhn S, Wille H, Nixon R, Dearmond SJ, Smart EJ, Anderson RG, Taraboulos A, Prusiner SB (1996) Subcellular colocalization of the cellular and scrapie prion proteins in caveolae-like membranous domains. Proc Natl Acad Sci USA 93:14945–14949
14. Naslavsky N, Stein R, Yanai A, Friedlander G, Taraboulos A (1997) Characterization of detergent-insoluble complexes containing the cellular prion protein and its scrapie isoform. J Biol Chem 272:6324–6331
15. Simons K, Ehehalt R (2002) Cholesterol, lipid rafts, and disease. J Clin Invest 110:597–603
16. Mulder M (2009) Sterols in the central nervous system. Curr Opin Clin Nutr Metab Care 12:152–158
17. Ikonen E (2008) Cellular cholesterol trafficking and compartmentalization. Nat Rev Mol Cell Biol 9:125–138
18. Watari H, Blanchette-Mackie EJ, Dwyer NK, Glick JM, Patel S, Neufeld EB, Brady RO, Pentchev PG, Strauss JF (1999) Niemann-Pick C1 protein: obligatory roles for N-terminal domains and lysosomal targeting in cholesterol mobilization. Proc Natl Acad Sci USA 96:805–810
19. Neufeld EB, Wastney M, Patel S, Suresh S, Cooney AM, Dwyer NK, Roff CF, Ohno K, Morris JA, Carstea ED, Incardona JP, Strauss JF, Vanier MT, Patterson MC, Brady RO, Pentchev PG, Blanchette-Mackie EJ (1999) The Niemann-Pick C1 protein resides in a vesicular compartment linked to retrograde transport of multiple lysosomal cargo. J Biol Chem 274:9627–9635
20. Vanier MT, Millat G (2003) Niemann-Pick disease type C. Clin Genet 64:269–281
21. Taraboulos A, Scott M, Semenov A, Avrahami D, Laszlo L, Prusiner SB (1995) Cholesterol depletion and modification of COOH-terminal targeting sequence of the prion protein inhibit formation of the scrapie isoform. J Cell Biol 129:121–132
22. Bate C, Salmona M, Diomede L, Williams A (2004) Squalestatin cures prion-infected neurons and protects against prion neurotoxicity. J Biol Chem 279:14983–14990
23. Gilch S, Kehler C, Schatzl HM (2006) The prion protein requires cholesterol for cell surface localization. Mol Cell Neurosci 31:346–353
24. Prior M, Lehmann S, Sy MS, Molloy B, McMahon HE (2007) Cyclodextrins inhibit replication of scrapie prion protein in cell culture. J Virol 81:11195–11207
25. Marella M, Lehmann S, Grassi J, Chabry J (2002) Filipin prevents pathological prion protein accumulation by reducing endocytosis and inducing cellular PrP release. J Biol Chem 277:25457–25464
26. Mange A, Nishida N, Milhavet O, McMahon HE, Casanova D, Lehmann S (2000) Amphotericin B inhibits the generation of the scrapie isoform of the prion protein in infected cultures. J Virol 74:3135–3140
27. Kaneko K, Vey M, Scott M, Pilkuhn S, Cohen FE, Prusiner SB (1997) COOH-terminal sequence of the cellular prion protein directs subcellular trafficking and controls conversion into the scrapie isoform. Proc Natl Acad Sci USA 94:2333–2338
28. Kempster S, Bate C, Williams A (2007) Simvastatin treatment prolongs the survival of scrapie-infected mice. Neuroreport 18:479–482
29. Mok SW, Thelen KM, Riemer C, Bamme T, Gultner S, Lutjohann D, Baier M (2006) Simvastatin prolongs survival times in prion infections of the central nervous system. Biochem Biophys Res Commun 348:697–702
30. Haviv Y, Avrahami D, Ovadia H, Ben Hur T, Gabizon R, Sharon R (2008) Induced neuroprotection independently from PrPSc

accumulation in a mouse model for prion disease treated with simvastatin. Arch Neurol 65:762–775
31. Adjou KT, Demaimay R, Lasmezas C, Deslys JP, Seman M, Dormont D (1995) MS-8209, a new amphotericin B derivative, provides enhanced efficacy in delaying hamster scrapie. Antimicrob Agents Chemother 39:2810–2812
32. Adjou KT, Demaimay R, Lasmezas CI, Seman M, Deslys JP, Dormont D (1996) Differential effects of a new amphotericin B derivative, MS-8209, on mouse BSE and scrapie: implications for the mechanism of action of polyene antibiotics. Res Virol 147:213–218
33. Lusa S, Blom TS, Eskelinen EL, Kuismanen E, Mansson JE, Simons K, Ikonen E (2001) Depletion of rafts in late endocytic membranes is controlled by NPC1-dependent recycling of cholesterol to the plasma membrane. J Cell Sci 114:1893–1900
34. Sobo K, LeBlanc I, Luyet PP, Fivaz M, Ferguson C, Parton RG, Gruenberg J, van der Goot FG (2007) Late endosomal cholesterol accumulation leads to impaired intra-endosomal trafficking. PLoS ONE 2:e851
35. Simons K, Gruenberg J (2000) Jamming the endosomal system: lipid rafts and lysosomal storage diseases. Trend Cell Biol 10:459–462
36. Koh CHV, Whiteman M, Li QX, Halliwell B, Jenner AM, Wong BS, Laughton KM, Wenk M, Masters CL, Beart PM, Bernard O, Cheung NS (2006) Chronic exposure to U18666A is associated with oxidative stress in cultured murine cortical neurons. J Neurochem 98:1278–1289
37. Lange Y, Ye J, Rigney R, Steck T (2000) Cholesterol movement in Niemann-Pick type C cells and in cells treated with amphiphiles. J Biol Chem 275:17468–17475
38. Runz H, Rietdorf J, Tomic I, de Bernard M, Beyreuther K, Pepperkok R, Hartmann T (2002) Inhibition of intracellular cholesterol transport alters presenilin localization and amyloid precursor protein processing in neuronal cells. J Neurosci 22:1679–1689
39. Ertmer A, Gilch S, Yun SW, Flechsig E, Klebl B, Stein-Gerlach M, Klein MA, Schatzl HM (2004) The tyrosine kinase inhibitor STI571 induces cellular clearance of PrPSc in prion-infected cells. J Biol Chem 279:41918–41927
40. Gilch S, Winklhofer KF, Groschup MH, Nunziante M, Lucassen R, Spielhaupter C, Muranyi W, Riesner D, Tatzelt J, Schatzl HM (2001) Intracellular re-routing of prion protein prevents propagation of PrP(Sc) and delays onset of prion disease. EMBO J 20:3957–3966
41. Schatzl HM, Laszlo L, Holtzman DM, Tatzelt J, Dearmond SJ, Weiner RI, Mobley WC, Prusiner SB (1997) A hypothalamic neuronal cell line persistently infected with scrapie prions exhibits apoptosis. J Virol 71:8821–8831
42. Gilch S, Wopfner F, Renner-Muller I, Kremmer E, Bauer C, Wolf E, Brem G, Groschup MH, Schatzl HM (2003) Polyclonal anti-PrP auto-antibodies induced with dimeric PrP interfere efficiently with PrPSc propagation in prion-infected cells. J Biol Chem 278:18524–18531
43. Cenedella RJ, Jacob R, Borchman D, Tang D, Neely AR, Samadi A, Mason RP, Sexton P (2004) Direct perturbation of lens membrane structure may contribute to cataracts caused by U18666A, an oxidosqualene cyclase inhibitor. J Lipid Res 45:1232–1241
44. Gilch S, Krammer C, Schatzl HM (2008) Targeting prion proteins in neurodegenerative disease. Expert Opin Biol Ther 8:923–940
45. Ganley IG, Pfeffer SR (2006) Cholesterol accumulation sequesters Rab9 and disrupts late endosome function in NPC1-deficient cells. J Biol Chem 281:17890–17899
46. Maxfield FR, Tabas I (2005) Role of cholesterol and lipid organization in disease. Nature 438:612–621
47. Klingenstein R, Lober S, Kujala P, Godsave S, Leliveld SR, Gmeiner P, Peters PJ, Korth C (2006) Tricyclic antidepressants, quinacrine and a novel, synthetic chimera thereof clear prions by destabilizing detergent-resistant membrane compartments. J Neurochem 98:748–759
48. Hagiwara K, Nakamura Y, Nishijima M, Yamakawa Y (2007) Prevention of prion propagation by dehydrocholesterol reductase inhibitors in cultured cells and a therapeutic trial in mice. Biol Pharm Bull 30:835–838
49. Avrahami D, Dayan-Amouyal Y, Tal S, Mincberg M, Davis C, Abramsky O, Gabizon R (2008) Virus-induced alterations of membrane lipids affect the incorporation of PrP(Sc) into cells. J Neurosci Res 86:2753–2762
50. Clague MJ, Urbe S, Aniento F, Gruenberg J (1994) Vacuolar ATPase activity is required for endosomal carrier vesicle formation. J Biol Chem 269:21–24
51. Borchelt DR, Taraboulos A, Prusiner SB (1992) Evidence for synthesis of scrapie prion proteins in the endocytic pathway. J Biol Chem 267:16188–16199
52. Beranger F, Mange A, Goud B, Lehmann S (2002) Stimulation of PrP(C) retrograde transport toward the endoplasmic reticulum increases accumulation of PrP(Sc) in prion-infected cells. J Biol Chem 277:38972–38977
53. Pacheco CD, Lieberman AP (2007) Lipid trafficking defects increase Beclin-1 and activate autophagy in Niemann-Pick type C disease. Autophagy 3:487–489
54. Sarkar S, Davies JE, Huang ZB, Tunnacliffe A, Rubinsztein DC (2007) Trehalose, a novel mTOR-independent autophagy enhancer, accelerates the clearance of mutant huntingtin and alpha-synuclein. J Biol Chem 282:5641–5652
55. Aguib Y, Heiseke A, Gilch S, Riemer C, Baier M, Schatzl HM, Ertmer A (2009) Autophagy induction by trehalose counteracts cellular prion infection. Autophagy 5:361–369
56. Heiseke A, Aguib Y, Riemer C, Baier M, Schatzl HM (2009) Lithium induces clearance of protease resistant prion protein in prion-infected cells by induction of autophagy. J Neurochem 109:25–34
57. Liao G, Yao Y, Liu J, Cheung S, Xie A (2007) Autophagic-lysosomal dysfunction is associated with cholesterol accumulation and neurodegeneration in NPC1−/− mice. J Neurochem 102:1–36
58. Pimpinelli F, Lehmann S, Maridonneau-Parini I (2005) The scrapie prion protein is present in flotillin-1-positive vesicles in central- but not peripheral-derived neuronal cell lines. Eur J Neurosci 21:2063–2072
59. McKinley MP, Taraboulos A, Kenaga L, Serban D, Stieber A, Dearmond SJ, Prusiner SB, Gonatas N (1991) Ultrastructural localization of scrapie prion proteins in cytoplasmic vesicles of infected cultured cells. Lab Invest 65:622–630
60. Borchelt DR, Scott M, Taraboulos A, Stahl N, Prusiner SB (1990) Scrapie and cellular prion proteins differ in their kinetics of synthesis and topology in cultured cells. J Cell Biol 110:743–752
61. Luhr KM, Nordstrom EK, Low P, Kristensson K (2004) Cathepsin B and L are involved in degradation of prions in GT1-1 neuronal cells. Neuroreport 15:1663–1667
62. Luhr KM, Nordstrom EK, Low P, Ljunggren HG, Taraboulos A, Kristensson K (2004) Scrapie protein degradation by cysteine proteases in CD11c + dendritic cells and GT1-1 neuronal cells. J Virol 78:4776–4782
63. Choudhury A, Sharma DK, Marks DL, Pagano RE (2004) Elevated endosomal cholesterol levels in Niemann-Pick cells inhibit Rab4 and perturb membrane recycling. Mol Biol Cell 15:4500–4511
64. Zerial M, McBride H (2001) Rab proteins as membrane organizers. Nat Rev Mol Cell Biol 2:107–117

65. Narita K, Choudhury A, Dobrenis K, Sharma DK, Holicky EL, Marks DL, Walkley SU, Pagano RE (2005) Protein transduction of Rab9 in Niemann-Pick C cells reduces cholesterol storage. Faseb J 19:1558–1560
66. Andersen OM, Reiche J, Schmidt V, Gotthardt M, Spoelgen R, Behlke J, von Arnim CAF, Breiderhoff T, Jansen P, Wu X, Bales KR, Cappai R, Masters CL, Gliemann J, Mufson EJ, Hyman BT, Paul SM, Nykjaer A, Willnow TE (2005) Neuronal sorting protein-related receptor sorLA/LR11 regulates processing of the amyloid precursor protein. Proc Natl Acad Sci USA 102:13461–13466